Upper Extremity Joint Torque Estimation Through an Electromyography-Driven Model

Shadman Tahmid
Human-Centric Design Research Lab,
Department of Mechanical Engineering,
Texas Tech University,
Lubbock, TX 79409
e-mail: shadman.tahmid@ttu.edu

Josep M. Font-Llagunes
Biomechanical Engineering Lab,
Department of Mechanical Engineering and
Research Centre for Biomedical Engineering,
Universitat Politècnica de Catalunya,
Barcelona, Catalonia 08034, Spain;
Health Technologies and Innovation,
Institut de Recerca Sant Joan de Deu,
Esplugues de Llobregat,
Catalonia, Spain
e-mail: josep.m.font@upc.edu

James Yang[1]
Human-Centric Design Research Lab,
Department of Mechanical Engineering,
Texas Tech University,
Lubbock, TX 79409
e-mail: james.yang@ttu.edu

Cerebrovascular accidents like a stroke can affect the lower limb as well as upper extremity joints (i.e., shoulder, elbow, or wrist) and hinder the ability to produce necessary torque for activities of daily living. In such cases, muscles' ability to generate forces reduces, thus affecting the joint's torque production. Understanding how muscles generate forces is a key element to injury detection. Researchers have developed several computational methods to obtain muscle forces and joint torques. Electromyography (EMG) driven modeling is one of the approaches to estimate muscle forces and obtain joint torques from muscle activity measurements. Musculoskeletal models and EMG-driven models require necessary muscle-specific parameters for the calculation. The focus of this study is to investigate the EMG-driven approach along with an upper extremity musculoskeletal model to determine muscle forces of two major muscle groups, biceps brachii and triceps brachii, consisting of seven muscle-tendon units. Estimated muscle forces are used to determine the elbow joint torque. Experimental EMG signals and motion capture data are collected for a healthy subject. The musculoskeletal model is scaled to match the geometric parameters of the subject. Then, the approach calculates muscle forces and joint moment for two tasks: simple elbow flexion extension and triceps kickback. Individual muscle forces and net joint torques for both tasks are estimated. The study also has compared the effect of muscle-tendon parameters (optimal fiber length and tendon slack length) on the estimated results. [DOI: 10.1115/1.4056255]

Keywords: joint torque, injury prediction, EMG, musculoskeletal model, upper extremity rehabilitation, human–computer interfaces/interactions

1 Introduction

The complex network of the central nervous system (CNS) conveys neural commands to upper and lower extremities. Being activated by neural signals, musculotendon units spanning a specific joint produce the necessary torque to actuate that joint. Actuation in upper and lower extremity joints together creates human movement. Brain injuries like stroke can damage this system, preventing the CNS from sending the necessary commands to generate muscle forces. Loss of muscle strength leads to loss in torque generation for upper and lower extremity joints and hinders patients' ability to do daily tasks. It is estimated one billion people around the world suffer from neurological disorders [1]. Complete recovery of functionality of the upper extremity in patients with neurological disorders is only 25% [2]. A recovering patient requires rehabilitation therapies to strengthen the injured muscles. Recent research indicates motion capture system can detect kinematic movement and provide necessary feedback to a specific rehabilitation task [3]. Additionally, estimating muscle forces as well as joint torques is important to quantify the muscle recovery of a patient. Researchers developed neuromusculoskeletal models to find muscle-tendon functions and replicate human movements. Determining joint torques from these models has been one of the major challenges. Inverse dynamics is one way of estimating joint torque from given movement data [4]. However, multiple muscle-tendon units about a single joint create a redundancy that leads to indeterminacy in muscle force calculation from joint torques. To solve this redundant issue, an optimization approach based on an objective function is required to calculate the individual muscle forces [5]. Another approach to estimating the muscle forces is through electromyography (EMG) signals. Nerve stimulation of muscle can be measured as an electrical activity directly from the muscle. Surface EMGs measure this neural activity from surface muscles during human movement [6]. With measured EMG signals, joint torques can be computed without [7–11] or with [12–20] a musculoskeletal model. Estimating joint torque with EMG signals only (no musculoskeletal model) usually requires additional dynamometers or force plates during the experimental data collection [7,9]. Musculoskeletal models along with experimentally derived EMG data were used by researchers to simulate upper [21] and lower extremity movements [13–16]. EMG signals recorded from muscles around a specific joint drove the muscle-tendon units of the musculoskeletal model through a forward dynamics approach [20]. Individual muscle forces were determined first with subject-specific muscle parameters (peak isometric force of the muscle, muscle pennation angle, tendon slack length, and optimal muscle fiber length) and kinematics-based variables (muscle-tendon length, muscle-tendon velocity, and moment arms). Subject-specific scaled musculoskeletal models can provide these parameters from motion capture data processed by inverse kinematics (IK) tool. OpenSim is one popular open-source platform to run simulations using these musculoskeletal models [22]. Estimated muscle forces can be used to determine joint torques according to the model equations of motion which avoid the necessity of an optimization-based approach.

Musculoskeletal models require muscle-tendon parameters like maximum isometric force, tendon slack length, and optimal fiber length to determine muscle forces. These parameters may vary depending on the subject's anthropometry, sex, or age [23]. True

[1]Corresponding author.
Contributed by the Computers and Information Division of ASME for publication in the Journal of Computing and Information Science in Engineering. Manuscript received July 26, 2022; final manuscript received November 7, 2022; published online December 9, 2022. Assoc. Editor: Caterina Rizzi.

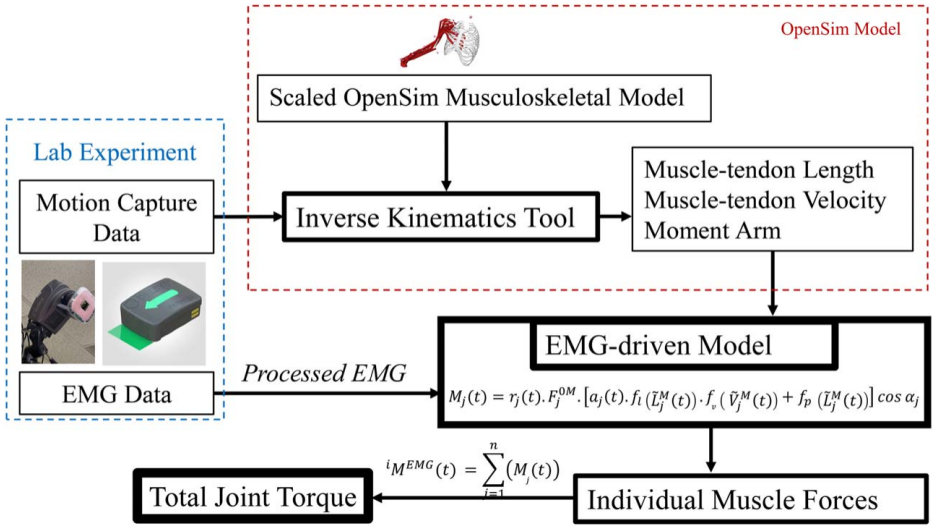

Fig. 1 Flowchart of the method

subject-specific determination of these parameters requires cadaveric specimen and is impossible to obtain from a living subject. A generic assumption in the literature can be noticed where the parameters were taken from multiple cadaveric measurements [24]. Often this approach failed to estimate an accurate representation of muscle-tendon force due to the high sensitivity to these parameters [25]. Scaling the muscle-tendon parameters to a specific subject improves this estimation of muscle force as well as joint moment. There are several ways existing in the literature that scale these parameters, especially optimal fiber length and tendon slack length. For example, OpenSim scales these two parameters by simply keeping their ratio constant for a specific joint angle to match the muscle-tendon unit length of the subject [22]. Another approach is to optimize the differences in generic and scaled models for a discrete number of joint angles [25]. Cerebrovascular accidents like stroke can affect the lower limb as well as upper extremity joints. Shoulder, elbow, or wrist can be affected and hinder the ability to produce necessary torque for activities of daily living (ADLs) [26]. Patients may require physiotherapy to rehabilitate and improve their ability to perform daily tasks. Digital human modeling is being employed to predict human motion and plan necessary rehabilitation techniques [3,27]. EMG-driven modeling can estimate these muscle forces and quantify any loss of movement of the affected limb.

Most of the aforementioned studies were focused on the lower extremity. This study explores joint torque estimation of the upper extremity through EMG data on the targeted muscles, i.e., the EMG-driven approach with an upper extremity OpenSim model to determine muscle forces for two specific elbow exercises (elbow flexion extension and triceps kickback). Muscle forces obtained by two major muscle groups (biceps brachii and triceps brachii) consisting of seven muscle-tendon units will be compared during this study. A pilot investigation was reported in Ref. [28]. Estimated muscle forces were used to determine joint torque produced by the elbow joint. Muscle parameters like optimal fiber length and tendon slack length in the pilot study were adapted from the literature. This study further explores the effect of anthropometry-based scaling of those parameters on the joint torque calculation.

2 Methodology

Figure 1 shows the flowchart for the methodology implemented in this research. The process starts with in-lab experimental data collection that obtains motion capture data of the movement and EMG signals of the target muscles. Obtained motion capture data go through the IK tool of OpenSim along with musculoskeletal model [29] to provide muscle-tendon length, muscle-tendon velocity, and moment arm for specific muscles. These parameters along with processed EMG signals are taken as inputs for the EMG-driven model that computes individual muscle forces. Once the individual muscle-generated moment of a joint is calculated, the total joint moment for a specific degrees-of-freedom (DOF) is obtained through the summation of all individual muscles' contributions. Details about these steps are described in the following sections.

2.1 Electromyography-Driven Model.

Joint moment contribution of a certain muscle is determined from Hill-type muscle models using Eqs. (1a) and (1b) [20].

$$M_j(t) = r_j(t).\, F_j^{0M}.\, a_j(t).f_l(\tilde{L}_j^M(t)).f_v\,(\tilde{V}_j^M(t)) + f_p\,(\tilde{L}_j^M(t))\cos\alpha_j \tag{1a}$$

$$l_j^{MT}(t) = l_j^M(t)\cos\alpha_j + l_j^T(t) \tag{1b}$$

where M_j is the moment about a given joint produced by the jth muscle, r_j is the moment arm of that muscle, F_j^{0M} is the peak isometric force, a_j is the muscle's activation obtained from the EMG signals, α_j is the muscle pennation angle, and $\tilde{L}_j^M$ and $\tilde{V}_j^M$ are the normalized muscle fiber length and velocity, respectively. $f_l(\tilde{L}_j^M(t))$, $f_v(\tilde{V}_j^M(t))$, and $f_p(\tilde{L}_j^M(t))$ represent the normalized muscle active force-length, passive force-length, and force-velocity curves, respectively (Fig. 2). Hill-type muscle models describe muscle-tendon length l_j^{MT} as shown in Eq. (1b), where l_j^M is the muscle fiber length and l_j^T is the tendon length for the jth muscle.

Normalized lengths $\tilde{L}_j^M(t)$ and $\tilde{L}_j^T(t)$, and velocity $\tilde{V}_j^M(t)$ are calculated from Eqs. (2a) and (2b). Here, v_j^{MT} is the muscle-tendon velocity, l_j^{ST} is the tendon slack length, and l_j^{0M} is the optimal muscle fiber length of the jth muscle [20].

$$\tilde{L}_j^M(t) = \frac{l_j^{MT}(t) - l_j^{ST}}{l_j^{0M}\cos\alpha_j} \tag{2a}$$

$$\tilde{V}_j^M(t) = \frac{v_j^{MT}(t)}{10\, l_j^{0M}} \tag{2b}$$

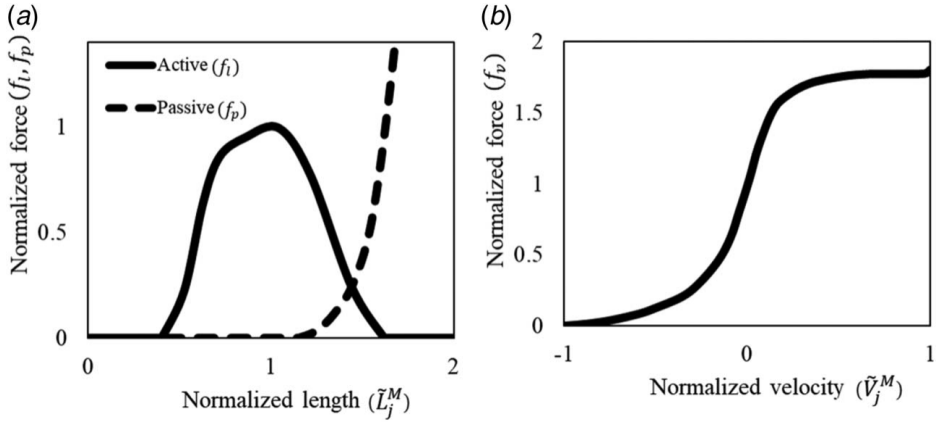

Fig. 2 (a) Normalized force-length relation to determine active force f_l and passive force f_p and (b) normalized force-velocity relation to determine f_v [20,29]

$$\tilde{L}_j^T(t) = \frac{l_j^T(t)}{l_j^{ST}} \tag{2c}$$

Once the individual muscle moment of a joint is calculated, the total joint moment for the ith DOF, ${}^iM^{EMG}(t)$, is obtained through summation of all individual muscle contributions at the ith DOF in Eq. (3), where n represents total number of muscles spanning that DOF.

$${}^iM^{EMG}(t) = \sum_{j=1}^{n} ({}^iM_j(t)) \tag{3}$$

2.2 Experimental Data Collection. A healthy 30-year-old male subject (mass 103 kg, height 188.1 cm) performed two different tasks that require the elbow to produce torques. Task 1 was simple elbow flexion extension. During this task, the shoulder was kept fixed at a 30 deg humerothoracic elevation. Task 2 was a standard muscle exercise called triceps kickback. Both tasks were performed without any loads in hand. Five trials per task were performed by the subject. The experimental protocol was approved by the Internal Review Board (IRB) at Texas Tech University.

The motion capture system was comprised of eight Eagle-4 cameras with ten retro-reflective markers placed on the right arm during each task as shown in Fig. 3 (Motion Analysis Corporation, Rohnert Park, CA). Details on the motion capture environment are explained in Refs. [30,31]. Analog EMG signals were recorded with Trigno Wireless Biofeedback System (DELSYS Incorporated, Natick, MA) containing 16 surface EMG sensors. To calculate muscle forces through EMG, three sensors were placed on the biceps brachii, long head of triceps muscle, and lateral head of triceps muscle. To make the study simple, biceps long and short head, brachialis (BRA), and brachioradialis (BRD) muscles shared the same EMG activation [29]. Similarly, triceps medial adopted the same activity as triceps lateral.

EMG placement and surface preparation were done according to guidelines established in Ref. [32]. To reduce active noises, any excessive hair from the skin surface was trimmed. An alcohol swab was applied to remove surface oils and other contaminants. Motion capture (60 Hz) and analog EMG (1299 Hz) were recorded simultaneously during each task using Cortex (Motion Analysis Corporation, CA). At first, a static standing T-pose trial was performed to be used for scaling purposes in OpenSim. Next, maximum voluntary contraction (MVC) was recorded for each of the target muscles [32]. These MVCs were later used to normalize the EMG data. After a 15 min rest, the subject was instructed to perform the tasks. Between each trial, a 5 min rest period was assigned. For each task, the subject's upper body was kept straight.

The markers in motion capture data were labeled and filtered at cut off 6 Hz frequency in Cortex (Motion Analysis Corporation, CA) [29] (Fig. 4). EMG post-process was done using Visual-3D (C-MOTION, Washington DC). Steps involved in processing the EMG data are shown in Fig. 5. EMG signals are recorded by placing electrodes on the skin. With activation of the muscle, skin, and electrodes also makes a small movement inducing noise to the signals [33]. EMG processing removes unwanted noise. EMG post-process was done using Visual-3D (C-MOTION, Washington DC). Raw EMG data were first high pass filtered (cut off 50 Hz) to remove high frequency noise and prevent influencing the signal. Then a full wave rectification was done to make the signals all positive. The EMG signals vary in both positive and negative polarities. Thus, the mean of the signals will always be zero and the mean value cannot be used as an indicator of the EMG amplitude unless the signal is rectified. The rectified signal was then low pass filtered with cut off frequency of 6 Hz to make the result look like the "envelope" of the original signal [12]. A fourth-order Butterworth filter smoothed out the data. Once processed, EMG data were normalized using MVC data collected for each muscle.

2.3 OpenSim Biomechanical Model. Moment calculation implemented in Eq. (1a) requires muscle-tendon length (l_j^{MT}), muscle-tendon velocity (v_j^{MT}), and moment arm (r_j) for the jth muscle. A generic upper extremity OpenSim musculoskeletal model was used for this step as shown in Fig. 6 [29]. The model includes seven DOF: three at the shoulder, two at the elbow, and two at the wrist. The joints are actuated by 50 Hill-type muscle-tendon units crossing the shoulder, elbow, forearm, and wrist [34].

The first step is to scale the model to anthropometrically match the human subject. Static marker data along with the subject's body mass scale the body segments, muscle actuators, and inertial properties of the model.

The IK tool in OpenSim calculates joint kinematics by tracking marker positions from experimental data. This tool minimizes the squared error between model markers and experimental markers' positions and provides an optimal joint angle for each frame [29]. As tasks in the experiment do not require shoulder or wrist movements, those coordinates in the model are locked. Time-dependent variables such as muscle-tendon length ($l_j^{MT}(t)$), muscle-tendon velocities ($v_j^{MT}(t)$), and moment arms ($r_j(t)$) are recorded in this step. Time invariant muscle parameters are taken as constant at first [29,35–38] as listed in Table 1. These muscle parameters are usually derived from multiple cadaveric specimens, making them acceptable for a wide range of subjects. Later optimal fiber length and tendon slack length are optimized to subject's anthropometry as described in Sec. 2.4.

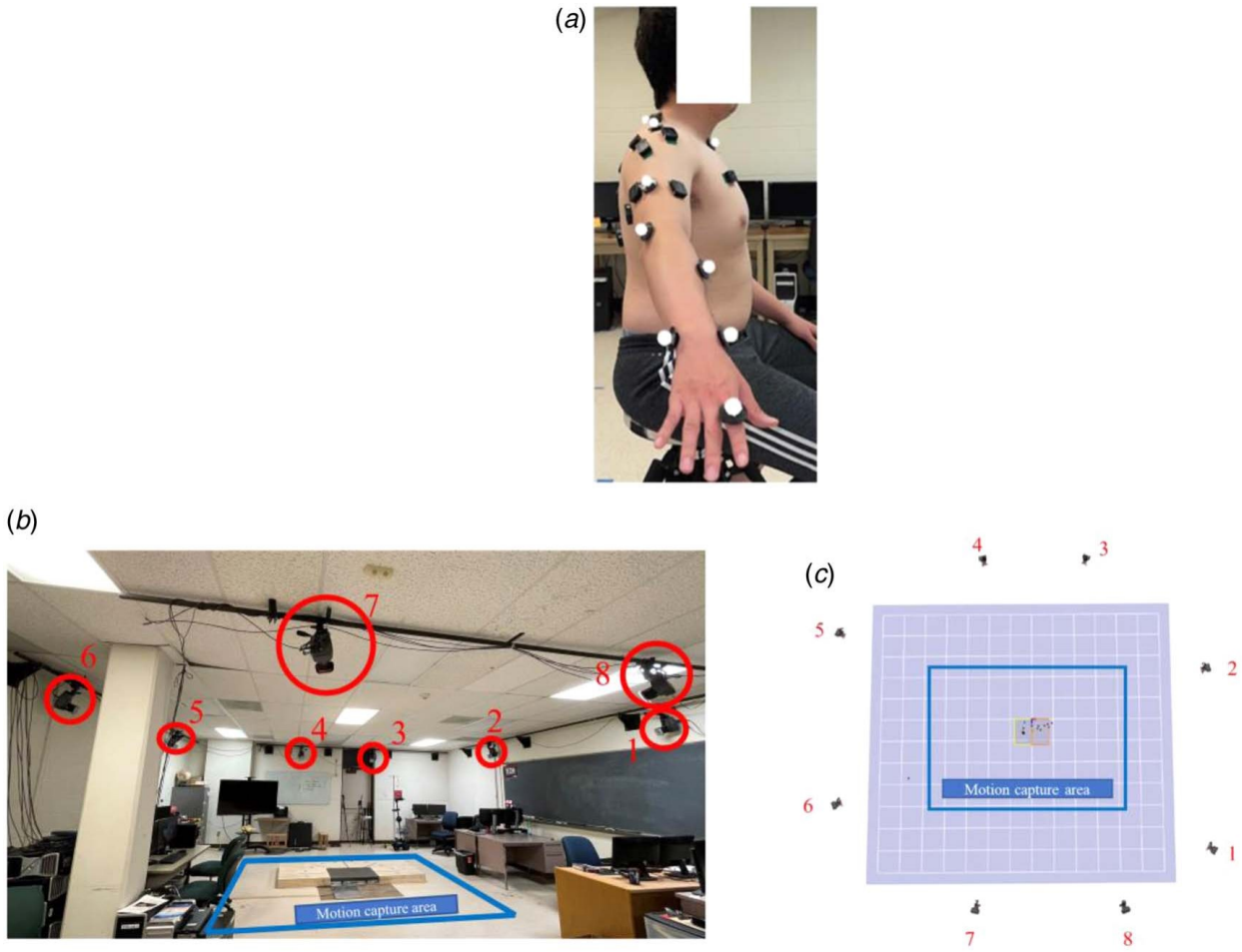

Fig. 3 Lab experiments: (a) motion capture marker and EMG placement for the subject, (b) motion capture environment with eight camera system, and (c) camera layout

2.4 Optimized Muscle Parameters to Subject's Anthropometry. Optimal fiber length (l_j^{0M}) and tendon slack length (l_j^{ST}) of a specific jth muscle are scaled to the subject's anthropometry according to the methods described by Modenese et al. [25]. With this method, muscle length and tendon length are first normalized according to Eqs. (2a) and (2c). Equation (1b) can further be expressed in terms of normalized muscle fiber length and normalized tendon length in Eq. (3).

$$l_j^{MT} = (\tilde{L}_j^{M} \cos\alpha) l_j^{0M} + \tilde{L}_j^{T} l_j^{ST} \quad (4)$$

Unscaled upper extremity dynamic model [29] is chosen for this step and named as "reference model". Optimal fiber length and tendon slack length for this model are assumed to be physiologically valid. Next, the reference model is scaled to the target subject's anthropometry and named "scaled model". l_j^{0M} and l_j^{ST} for this model need to be calculated. For both models, each DOF is uniformly sampled to m number of points (k = 1, 2, ..., m). For the kth pose, Eq. (3) can be rewritten in Eq. (4).

$$l_{j,k}^{MT} = (\tilde{L}_{j,k}^{M} \cos\alpha_j) l_j^{0M} + \tilde{L}_{j,k}^{T} l_j^{ST} \quad (5)$$

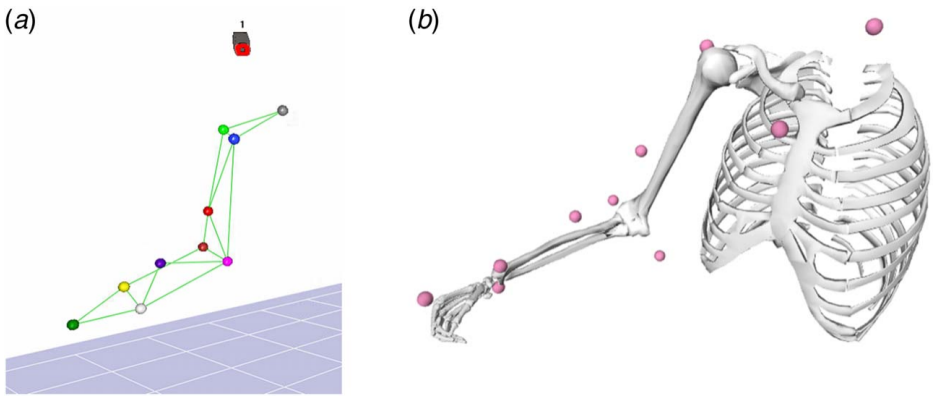

Fig. 4 (a) Processed motion capture data with ten markers and (b) corresponding marker position in the OpenSim upper extremity model [29]

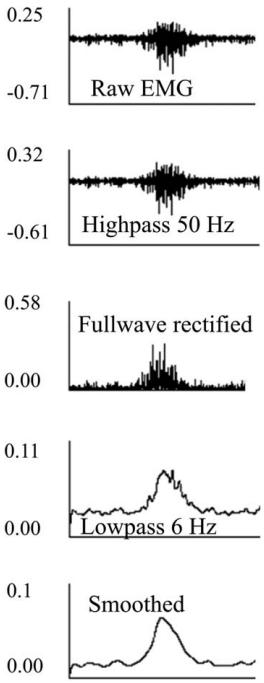

Fig. 5 Steps to process EMG signals for triceps long muscle for Task 2

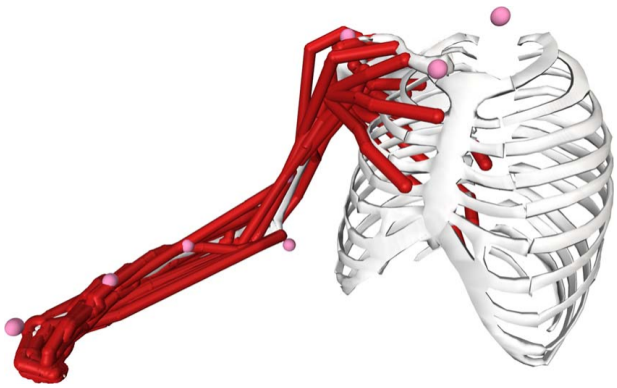

Fig. 6 OpenSim upper extremity model [29]. Lines around skeleton represent muscles in the musculoskeletal model.

$\tilde{L}^{M}_{j,k}$ and $\tilde{L}^{T}_{j,k}$ for all the sample points are calculated from the reference model ($L^{M}_{j,1}, L^{M}_{j,2}, \ldots, L^{M}_{j,k}$ and $L^{T}_{j,1}, L^{T}_{j,2}, \ldots, L^{T}_{j,k}$). Next, muscle-tendon lengths for all sample points are taken from the scaled model ($l^{MT}_{j,1}, l^{MT}_{j,2}, \ldots, l^{MT}_{j,k}$). Now Eq. (4) can be expressed

Table 1 Muscle parameters from the literature [29,35–38]

Muscle	l_j^{0M}(cm) [38]	F_j^{0M}(N) [36,37]	l_j^{ST}(cm) [29,35]	α_j (deg) [38]
Biceps long head	11.6	525.1	27.8	0
Biceps short head	13.2	316.8	20.0	0
Brachialis	8.6	1177.4	5.4	0
Brachioradialis	17.3	276.0	13.3	0
Triceps long head	13.4	771.8	14.3	12.0
Triceps lateral head	11.4	717.5	9.8	9.0
Triceps medial head (TRImed)	11.4	717.5	9.1	9.0

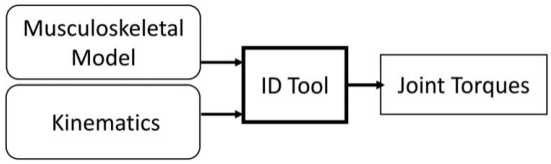

Fig. 7 Flowchart on how the ID tool works

as follows for all the poses.

$$l^{MT}_{j,1} = (\tilde{L}^{M}_{j,1} \cos \alpha_j) l^{0M}_j + \tilde{L}^{T}_{j,1} l^{ST}_j$$
$$l^{MT}_{j,2} = (\tilde{L}^{M}_{j,2} \cos \alpha_j) l^{0M}_j + \tilde{L}^{T}_{j,2} l^{ST}_j$$
$$\vdots$$
$$l^{MT}_{j,m} = (\tilde{L}^{M}_{j,m} \cos \alpha_j) l^{0M}_j + \tilde{L}^{T}_{j,m} l^{ST}_j$$

As the above equations generate an over constrained linear system, it is solved in least square sense to get the values of optimal fiber length (l^{0M}_j) and tendon slack length (l^{ST}_j) of the jth muscle.

2.5 Inverse Dynamics. In addition to EMG-driven modeling, joint torques were also obtained using OpenSim native inverse dynamics (ID) tool (Fig. 7). This tool determines net forces and torques for a joint based on provided kinematics. The scaled musculoskeletal model and kinematics were fed to the ID tool and the total joint torque of the elbow was calculated for both tasks. The range of joint torques obtained here will be compared with the results obtained from EMG-driven modeling.

3 Results

Figure 8(a) shows each muscle's moment of elbow joint for Task 1 using EMG-driven model. Among the muscles, biceps brachii group (long head and short head) shows higher levels of moments than the triceps group. Also, an upward trend can be noticed during flexion and a downward trend for extension of elbow. The total joint torque produced by all muscles for elbow flexion extension based on Eq. (3) is shown in Fig. 8(b). A peak moment of around 25 Nm is achieved at the end of elbow flexion. After the peak, the joint moment keeps decreasing during extension and finally reaches a fixed value of 5 Nm.

A typical triceps exercise (triceps kickback) is performed by the subject, where the same set of muscles is recorded through EMG shown in Fig. 9(a). Similar to Task 1, the biceps long head (BICLong) shows a peak moment of 8 Nm. Results show that triceps group (long head, lateral head, and medial head) generates negative moments throughout the task. Triceps long head (TRILong) has the highest negative moment of around −4 Nm. Summing up individual moments, Fig. 9(b) shows the net elbow joint torque. During Task 2, the joint moment reached a peak of 8 Nm.

Range of joint torques obtained from the ID tool in OpenSim and EMG-driven model are compared in Fig. 10. Results show good comparison between the techniques with Task 1 slightly closer to the ID results than Task 2.

4 Discussion

This study presented a method to integrate the EMG-driven model and musculoskeletal model to estimate elbow joint torque. Two major muscle groups containing seven muscle-tendon units crossing the elbow joint were used. Two different tasks were performed by the subject to collect necessary EMG and motion

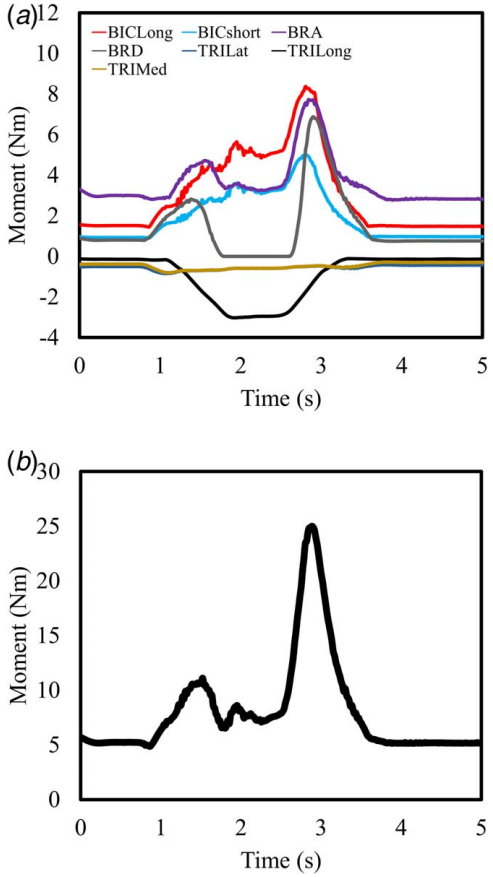

Fig. 8 Joint moment from Task 1: (a) produced by individual muscles and (b) total joint torque. BICLong: Biceps long head, BICshort: Biceps short head, BRA: Brachialis, BRD: Brachioradialis, TRILat: Triceps lateral head, TRILong: Triceps long head, TRImed: Triceps medial head.

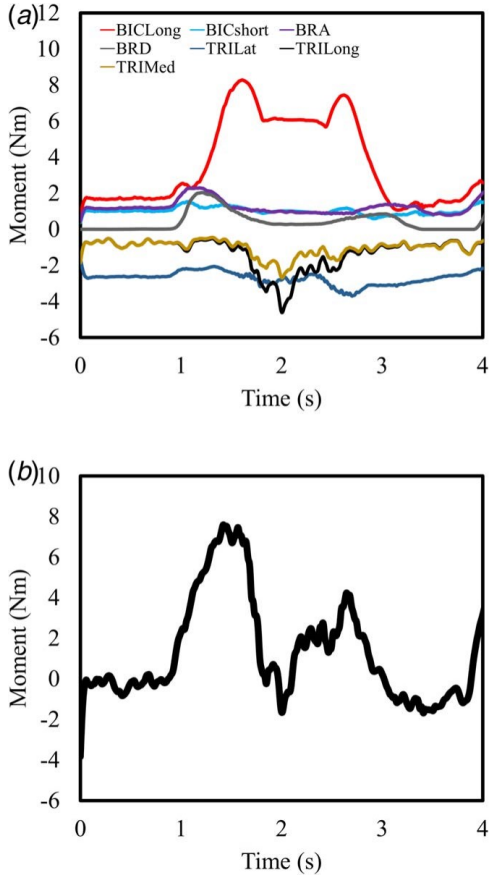

Fig. 9 Joint moment from Task 2: (a) produced by individual muscles and (b) total joint torque

capture data. Among the tasks, Task 1 with elbow flexion-extension without any load showed higher joint torque compared to Task 2. From Figs. 8(a) and 9(a), it was noticed for both tasks biceps brachii produced the highest moment, which agreed with the literature as biceps are the strongest flexors in the upper extremity [39].

EMG process and normalization play an important role in this approach. Several methods to normalize EMG signals exist. For example, some researchers took the maximum activation during a task as the reference value for normalization [20,40]. In this study, peak activation during MVC was taken as the reference to normalize muscle activation computed from EMG. Each muscle had different testing protocols to determine MVCs [32]. The differences in reference activation level affect EMG processing and may affect the joint torque calculation. Even though MVC reference for normalization obtained a good result for a healthy subject in this study, the question remains how to obtain this value for a patient who cannot perform necessary maximum contraction due to risk of injury, muscle inhibition, or pain. In our future research, we may try other normalization methods.

The moment calculation required several inputs from a musculoskeletal model. Muscle-tendon length, muscle-tendon velocities, and moment arm were recorded in this study as a function of joint angle. One of the important factors here was the geometric adjustment of the musculoskeletal model to reflect different subjects. OpenSim scaling with a static marker set was used. This process scaled the inertial properties, body segments, and muscle actuators geometry; but did not adjust the subject-specific muscle parameters like maximum isometric force or pennation angle. As determining subject-specific values of these parameters is complex, we adapted their values from the literature. A sensitivity test regarding these parameters may improve the estimation [29,35–37].

Time invariant muscle parameters listed in Table 1 were taken as constant during the preliminary study. Even though the parameters in the literature were calculated based on multiple cadaveric specimens, it is not ideal to assume each subject has the same value. Subject-specific parameters may vary due to different muscle architectures in different subjects. Since it is not possible to measure these in vivo in living subjects, optimization-based approaches

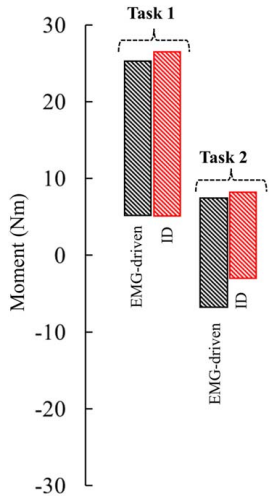

Fig. 10 Range of joint torque comparison for ID and EMG-driven modeling approach for both tasks

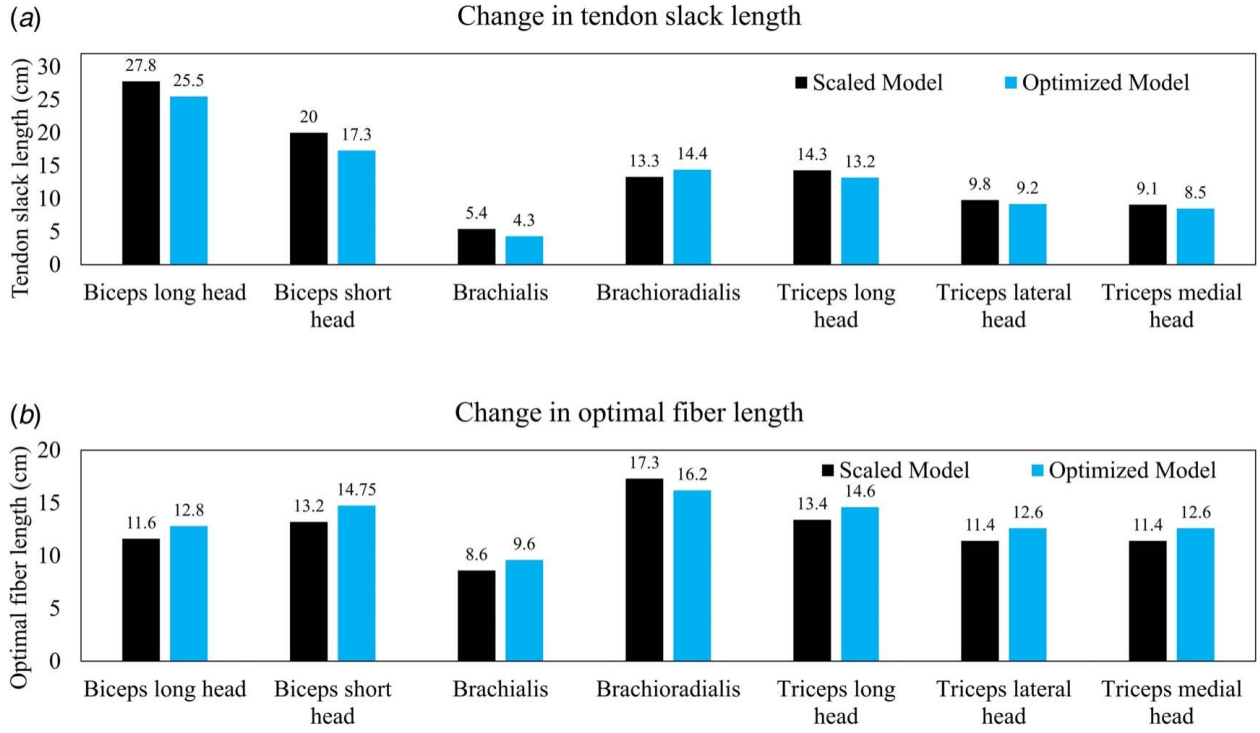

Fig. 11 Comparison of muscle parameters: (a) tendon slack length and (b) optimal fiber length between the scaled model and the optimized model

can estimate these parameters based on linear scaling of the model to subject. To further check the validity of these parameters, optimal fiber length and tendon slack length were optimized based on Modenese et al. [25], as explained in Sec. 2.4. This approach used anthropometry-based calculation to optimize the optimal fiber length and tendon slack length for multiple poses of the musculoskeletal model in different DOF. The results obtained are shown in Figs. 11(a) and 11(b). The previous model (only scaled, muscle parameters were taken from the literature) is called "scaled model" and the new muscle parameter optimized model is named as "optimized model". A maximum of 11.7% change in the optimal fiber length can be noticed in biceps short head (BICshort). Brachioradialis showed the smallest change of 6.7%. As for tendon slack length, brachialis shifted most with a 20.3% change and triceps lateral head (TRILat) had the lowest 6.1% shift.

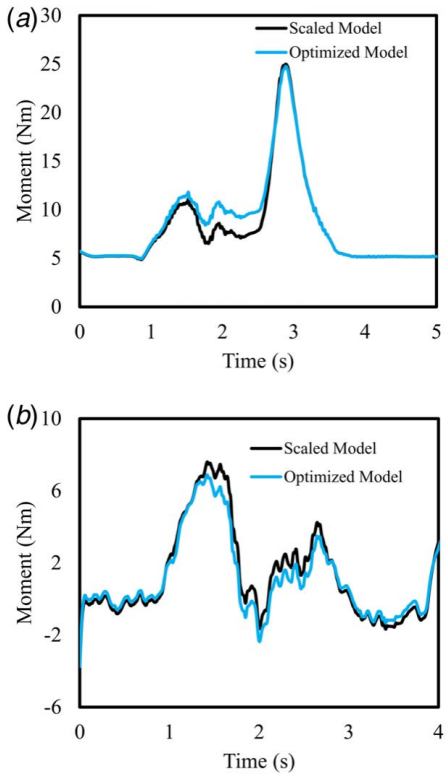

Fig. 12 Comparison of joint moment between the scaled model and optimized model for (a) Task 1 and (b) Task 2

Figure 12 shows a comparison between the joint moments predicted by the scaled model and optimized model for both tasks. Only the optimal fiber length and tendon slack length were optimized in this study as shown in Fig. 11. Joint moment calculated with the optimized parameters shows a little deviation during the flexion part of Task 1, whereas for extension, it remains similar. As for Task 2, small variations can be noticed during the overall task, but kept the same moment profile as the scaled model.

Another limitation of this study is the inability to obtain subject-specific peak isometric force for each muscle. This parameter is directly related to subjects' individual muscle volumes, which can be obtained through MRI scans of the specific subject. Therefore, we relied on the published literature to obtain these values [36,37]. An appropriate estimation of this parameter may improve the joint moment estimation for a specific subject.

Velocity and acceleration play an important role in dynamic joint torque calculations [41]. A previous study that compared static and dynamic joint torque for elbow found at lower speed (less than 0.25 rad/s) gravitational components contributed most to the joint torque [41]. But with the increase of velocity (more than 1 rad/s) and acceleration, Coriolis-centrifugal and inertial contributions became prominent [41]. As shown in Fig. 13, the angular velocity and acceleration reached a maximum of 3 rad/s and 12 rad/s, respectively. These high velocity and acceleration values (i.e., dynamic case) contributed to a high joint torque for Task 1.

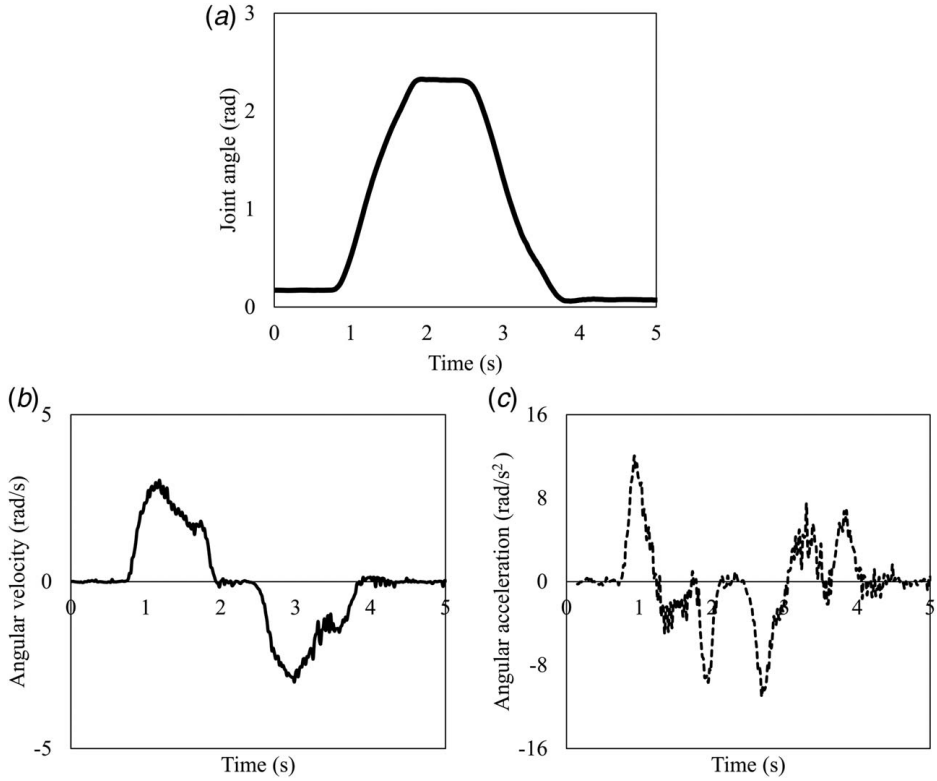

Fig. 13 (a) Joint angle, (b) angular velocity, and (c) angular acceleration for Task 1

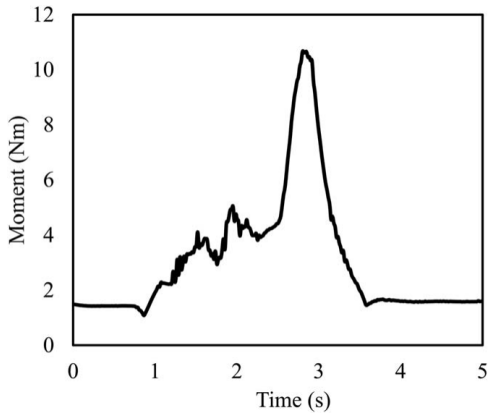

Fig. 14 Joint torque for Task 1 if BRA and BRD are not considered

EMG data from deep muscles like brachialis or brachioradialis could not be obtained as they are not accessible by surface EMG sensors. Some researchers used surface EMG to derive data from brachialis muscle [42], but the possible interference from the nearby muscles reduced the quality of the data [43]. Therefore, it was assumed in this study that brachialis and brachioradialis shared the same activity as biceps brachii [29]. This assumption might carry some errors in the calculation of joint torque, as in reality, their activation values might not be exactly the same. If the contributions from these two muscles were not considered, the maximum total joint torque for Task 1 would have been lowered (Fig. 14) to around 10 Nm, which agrees with experiments conducted by Peng et al. [44]. The inverse dynamics approach could calculate joint moments based on kinematics from motion capture data and does not require muscle forces. By optimizing the error difference of joint torque in these two methods (EMG-driven joint moment calculation and inverse dynamics), muscle excitation of those inaccessible muscles can be obtained [45]. This will be our future work.

5 Conclusion

This study reported a method to estimate joint torque from EMG data and a musculoskeletal model and apply this procedure to calculate the elbow joint moment. The EMG-driven model required some muscle-tendon parameter values like maximum isometric force, tendon slack length, pennation angle, and optimal muscle fiber length. Other time-dependent variables like muscle-tendon length, muscle-tendon velocity, moment arm around target joint and, most importantly, muscle activation from EMG data was also needed for the calculation. Kinematic time-dependent variables were calculated through a musculoskeletal model of the upper extremity. From motion capture data, the inverse kinematics tool in OpenSim was used to calculate the joint angles, thus obtaining muscle-tendon length, muscle-tendon velocity, and moment arm. EMG and motion capture data were collected for two specific tasks involving the elbow. Joint torques were calculated for both tasks and compared to each other. The method can be an important tool to assess muscle-related injuries of the upper extremity, e.g., for individuals with post-stroke.

Acknowledgment

This study was partly supported by National Science Foundation (CBET # 2014278) and US Army Medical Research and Development Command (USAMRDC) under Contract No. W81XWH18C0102.

Conflict of Interest

There are no conflicts of interest.

Data Availability Statement

No data, models, or code were generated or used for this paper.

References

[1] Lanzoni, D., Vitali, A., Regazzoni, D., and Rizzi, C., 2022, "Design of Customized Virtual Reality Serious Games for the Cognitive Rehabilitation of Retrograde Amnesia After Brain Stroke," ASME J. Comput. Inf. Sci. Eng., 22(3), p. 031009.

[2] Srimathveeravalli, G., Gourishankar, V., Kumar, A., and Kesavadas, T., 2009, "Experimental Evaluation of Shared Control for Rehabilitation of Fine Motor Skills," ASME J. Comput. Inf. Sci. Eng., 9(1), p. 014503.

[3] Vitali, A., Maffioletti, F., Regazzoni, D., and Rizzi, C., 2020, "Quantitative Assessment of Shoulder Rehabilitation Using Digital Motion Acquisition and Convolutional Neural Network," ASME J. Comput. Inf. Sci. Eng., 20(5), p. 054502.

[4] Bisseling, R. W., and Hof, A. L., 2006, "Handling of Impact Forces in Inverse Dynamics," J. Biomech., 39(13), pp. 2438–2444.

[5] Shourijeh, M. S., Mehrabi, N., and McPhee, J., 2017, "Forward Static Optimization in Dynamic Simulation of Human Musculoskeletal Systems: A Proof-of-Concept Study," ASME J. Comput. Nonlinear Dyn., 12(5), p. 051005.

[6] Farina, D., and Negro, F., 2012, "Accessing the Neural Drive to Muscle and Translation to Neurorehabilitation Technologies," IEEE Rev. Biomed. Eng., 5, pp. 3–14.

[7] Doorenbosch, C. A., and Harlaar, J., 2003, "A Clinically Applicable EMG–Force Model to Quantify Active Stabilization of the Knee After a Lesion of the Anterior Cruciate Ligament," Clin. Biomech., 18(2), pp. 142–149.

[8] Kellis, E., and Baltzopoulos, V., 1997, "The Effects of Antagonist Moment on the Resultant Knee Joint Moment During Isokinetic Testing of the Knee Extensors," Eur. J. Appl. Physiol. Occup. Physiol., 76(3), pp. 253–259.

[9] Amarantini, D., and Martin, L., 2004, "A Method to Combine Numerical Optimization and EMG Data for the Estimation of Joint Moments Under Dynamic Conditions," J. Biomech., 37(9), pp. 1393–1404.

[10] Liu, M. M., Herzog, W., and Savelberg, H. H., 1999, "Dynamic Muscle Force Predictions From EMG: An Artificial Neural Network Approach," J. Electromyogr. Kinesiol., 9(6), pp. 391–400.

[11] Olney, S. J., and Winter, D. A., 1985, "Predictions of Knee and Ankle Moments of Force in Walking From EMG and Kinematic Data," J. Biomech., 18(1), pp. 9–20.

[12] Lloyd, D. G., and Besier, T. F., 2003, "An EMG-Driven Musculoskeletal Model to Estimate Muscle Forces and Knee Joint Moments In Vivo," J. Biomech., 36(6), pp. 765–776.

[13] Bogey, R. A., Perry, J., and Gitter, A. J., 2005, "An EMG-to-Force Processing Approach for Determining Ankle Muscle Forces During Normal Human Gait," IEEE Trans. Neural Syst. Rehabil. Eng., 13(3), pp. 302–310.

[14] Sartori, M., Reggiani, M., Farina, D., and Lloyd, D. G., 2012, "EMG-Driven Forward-Dynamic Estimation of Muscle Force and Joint Moment About Multiple Degrees of Freedom in the Human Lower Extremity," PLoS One, 7(12), pp. e52618.

[15] Kumar, D., Rudolph, K. S., and Manal, K. T., 2012, "EMG-Driven Modeling Approach to Muscle Force and Joint Load Estimations: Case Study in Knee Osteoarthritis," J. Orthop. Res., 30(3), pp. 377–383.

[16] Buchanan, T. S., Lloyd, D. G., Manal, K., and Besier, T. F., 2005, "Estimation of Muscle Forces and Joint Moments Using a Forward-Inverse Dynamics Model," Med. Sci. Sports Exercise, 37(11), pp. 1911–1916.

[17] Winby, C. R., Lloyd, D. G., Besier, T. F., and Kirk, T. B., 2009, "Muscle and External Load Contribution to Knee Joint Contact Loads During Normal Gait," J. Biomech., 42(14), pp. 2294–2300.

[18] Gardinier, E. S., Manal, K., Buchanan, T. S., and Snyder-Mackler, L., 2013, "Minimum Detectable Change for Knee Joint Contact Force Estimates Using an EMG-Driven Model," Gait Posture, 38(4), pp. 1051–1053.

[19] Gerus, P., Rao, G., Buchanan, T. S., and Berton, E., 2010, "A Clinically Applicable Model to Estimate the Opposing Muscle Groups Contributions to Isometric and Dynamic Tasks," Ann. Biomed. Eng., 38(7), pp. 2406–2417.

[20] Meyer, A. J., Patten, C., and Fregly, B. J., 2017, "Lower Extremity EMG-Driven Modeling of Walking With Automated Adjustment of Musculoskeletal Geometry," PLoS One, 12(7), p. e0179698.

[21] Langenderfer, J., LaScalza, S., Mell, A., Carpenter, J. E., Kuhn, J. E., and Hughes, R. E., 2005, "An EMG-Driven Model of the Upper Extremity and Estimation of Long Head Biceps Force," Comput. Biol. Med., 35(1), pp. 25–39.

[22] Delp, S. L., Anderson, F. C., Arnold, A. S., Loan, P., Habib, A., John, C. T., and Thelen, D. G., 2007, "OpenSim: Open-Source Software to Create and Analyze Dynamic Simulations of Movement," IEEE Trans. Biomed. Eng., 54(11), pp. 1940–1950.

[23] Thelen, D. G., 2003, "Adjustment of Muscle Mechanics Model Parameters to Simulate Dynamic Contractions in Older Adults," ASME J. Biomech. Eng., 125(1), pp. 70–77.

[24] Stiver, M., Bradshaw, L., Breinhorst, E., Anne, A., and Mirjalili, S. A., 2021, "Three-Dimensional Muscle Architecture of the Infant and Adult Trapezius: A Cadaveric Pilot Study," Anatomy, 15(1), pp. 26–35.

[25] Modenese, L., Ceseracciu, E., Reggiani, M., and Lloyd, D. G., 2016, "Estimation of Musculotendon Parameters for Scaled and Subject Specific Musculoskeletal Models Using an Optimization Technique," J. Biomech., 49(2), pp. 141–148.

[26] Tahmid, S., Yang, J., and Font-Llagunes, J. M., 2019, "Review of Models and Robotic Devices for Stroke Survivors' Upper Extremity Rehabilitation," International Design Engineering Technical Conferences and Computers and Information in Engineering Conference, Hilton Anaheim, Anaheim, CA, Aug. 18–21.

[27] Kakizaki, T., Endo, M., Urii, J., and Endo, M., 2017, "Application of Digital Human Models to Physiotherapy Training," ASME J. Comput. Inf. Sci. Eng., 17(3), p. 031014.

[28] Tahmid, S., Font-Llagunes, J. M., and Yang, J., 2022, "Upper Extremity Joint Torque Estimation Through an EMG-Driven Model," International Design Engineering Technical Conferences and Computers and Information in Engineering Conference, St. Louis, MO, Aug. 14–17.

[29] Saul, K. R., Hu, X., Goehler, C. M., Vidt, M. E., Daly, M., Velisar, A., and Murray, W. M., 2015, "Benchmarking of Dynamic Simulation Predictions in Two Software Platforms Using an Upper Limb Musculoskeletal Model," Comput. Meth. Biomech. Biomed. Eng., 18(13), pp. 1445–1458.

[30] Xiang, Y., Tahmid, S., Owens, P., and Yang, J., 2021, "Single Task Optimization-Based Planar Box Delivery Motion Simulation and Experimental Validation," ASME J. Mech. Rob., 13(2), p. 024501.

[31] Xiang, Y., Tahmid, S., Owens, P., and Yang, J., 2020, "Two-Dimensional Symmetric Box Delivery Motion Prediction and Validation: Subtask-Based Optimization Method," Appl. Sci., 10(24), pp. 8798.

[32] Konrad, P., 2006, The ABC of EMG: A Practical Introduction to Kinesiological Electromyography, 1st ed., Noraxon Inc., Scottsdale, AZ.

[33] Chowdhury, R. H., Reaz, M. B., Ali, M. A. B. M., Bakar, A. A., Chellappan, K., and Chang, T. G., 2013, "Surface Electromyography Signal Processing and Classification Techniques," Sensors, 13(9), pp. 12431–12466.

[34] Schutte, L. M., 1993, "Using Musculoskeletal Models to Explore Strategies for Improving Performance in Electrical Stimulation-Induced Leg Cycle Ergometry," Ph.D. dissertation, Stanford University, Stanford, CA.

[35] Holzbaur, K. R., Murray, W. M., and Delp, S. L., 2005, "A Model of the Upper Extremity for Simulating Musculoskeletal Surgery and Analyzing Neuromuscular Control," Ann. Biomed. Eng., 33(6), pp. 829–840.

[36] Holzbaur, K. R., Murray, W. M., Gold, G. E., and Delp, S. L., 2007, "Upper Limb Muscle Volumes in Adult Subjects," J. Biomech., 40(4), pp. 742–749.

[37] Holzbaur, K. R., Delp, S. L., Gold, G. E., and Murray, W. M., 2007, "Moment-Generating Capacity of Upper Limb Muscles in Healthy Adults," J. Biomech., 40(11), pp. 2442–2449.

[38] Murray, W. M., Buchanan, T. S., and Delp, S. L., 2000, "The Isometric Functional Capacity of Muscles That Cross the Elbow," J. Biomech., 33(8), pp. 943–952.

[39] Youm, Y., Flatt, A. E., and Sprague, B. L., 1978, "Force Analysis of Elbow Flexors," Sixth New England Bioengineering Conference Sixth New England Bioengineering Conference, Kingston, RI, Mar. 23–24, pp. 55–59.

[40] Naik, G., 2012, Computational Intelligence in Electromyography Analysis-A Perspective on Current Applications and Future Challenges, Vol. 10, IntechOpen, London, UK, p. 175.

[41] Kodek, T., and Munih, M., 2003, "An Analysis of Static and Dynamic Joint Torques in Elbow Flexion-Extension Movements," Simul. Modell. Pract. Theory, 11(3–4), pp. 297–311.

[42] Praagman, M., Chadwick, E. K. J., Van der Helm, F. C. T., and Veeger, H. E. J., 2010, "The Effect of Elbow Angle and External Moment on Load Sharing of Elbow Muscles," J. Electromyogr. Kinesiol., 20(5), pp. 912–922.

[43] Staudenmann, D., and Taube, W., 2015, "Brachialis Muscle Activity can be Assessed With Surface Electromyography," J. Electromyogr. Kinesiol., 25(2), pp. 199–204.

[44] Peng, L., Hou, Z. G., and Wang, W., 2015, "A Dynamic EMG-Torque Model of Elbow Based on Neural Networks," 2015 37th Annual International Conference of the IEEE Engineering in Medicine and Biology Society (EMBC), Milan, Italy, Aug. 25–29, pp. 2852–2855.

[45] Ao, D., Shourijeh, M. S., Patten, C., and Fregly, B. J., 2020, "Evaluation of Synergy Extrapolation for Predicting Unmeasured Muscle Excitations From Measured Muscle Synergies," Front. Hum. Neurosci., 14, p. 588943.